JOURNAL OF BUILDING PHYSICS

Technical Note

Journal of Building Physics
1–12

DOI: 10.1177/1744259120914644
journals.sagepub.com/home/jen
SAGE

Reflective insulation assemblies for above-ceiling applications

Kah Wei Yam[1], Khar San Teh[1], Patrick Loi[2] and David W Yarbrough[3]

Abstract

Previously published hot-box data have been used to construct equations for the thermal resistance of enclosed reflective air spaces (reflective insulation assemblies) for a wide range of temperatures, air gap dimensions, thermal emittances, and heat flow directions. The thermal resistances or R-values (RSI) calculated with the equations compare favorably with previously published thermal resistances. Significant differences from relative strength index values (m^2 K/W) calculated using ISO 6946 were observed. Equations for calculating heat transfer coefficients for conduction–convection with constants for the heat flow directions up, 45° up, horizontal, 45° down, and down are contained in this article. The conduction–convection coefficient for planar air spaces oriented at any angle and heated above can be obtained by interpolation between heat flow down and heat flow at a downward angle of 45° or heat flow down at an angle of 45° and horizontal heat flow. The overall heat transfer coefficient is obtained by adding the thermal radiation contribution to the conduction–convection contribution. The relative strength index of enclosed reflective air spaces is the reciprocal of the overall heat transfer coefficient for the air space. This air space relative strength index is especially useful as input for the calculation of U-values for ceiling–roof assemblies located in hot climates.

Keywords

Reflective insulation, thermal resistance, enclosed reflective air spaces, low-emittance thermal insulation, inclined air spaces

[1]San Miguel Yamamura Woven Products, Air Keroh, Malaysia
[2]Propak Enterprise, Selangor, Malaysia
[3]R & D Services, Inc., Cookeville, TN, USA

Corresponding author:
David W Yarbrough, R & D Services, Inc., 102 Mill Drive, Cookeville, TN 38501-2175, USA.
Email: Dave@RDServices.com

Introduction

The subject of this article is relative strength index (RSI values (m^2 K/W) for heat flow as a function of angle (or roof slope). The results of interest are downward heat flow from horizontal surfaces (0°) to heat flow from a vertical surface (90°). A historically and technically significant evaluation of the thermal performance of enclosed air spaces was published by the US National Bureau of Standards (NBS; Robinson et al., 1954). The data in the NBS report consists of 96 guarded hot-box tests of panels with enclosed air spaces of uniform thickness. While the NBS research was not the earliest laboratory evaluation of enclosed reflective air spaces (Goss and Miller, 1989), the current definition of a reflective insulation assembly, it represents the first comprehensive evaluation of the thermal resistance of enclosed air spaces that include a low thermal emittance surface perpendicular to the heat flow direction. Heat flow down is emphasized to expedite the use of this technology in hot climates. The RSI data for downward heat flow interpolations for RSI are available in this article.

Research in the field of reflective insulations is well represented in the literature by a 1989 review with 105 references (Goss and Miller, 1989). In addition, there is an extensive review of research involving reflective insulations and radiant barriers (Lee et al., 2016), and numerical simulation work and correlations for reflective air spaces (Saber, 2014; Saber et al., 2020).

The NBS hot-box data were released in 1956 as Housing Research Paper 32 (HRP 32) by Robinson et al. (1954). Data from HRP 32 form the basis for the tables "Thermal Conductances and Resistances of a Plane Air Space" contained in an early edition of the American Society of Heating, Refrigerating and Air-Conditioning Engineers (ASHRAE) Handbook of Fundamentals (ASHRAE, 1972) and subsequent editions of the Handbook (ASHRAE, 2017). The NBS data set was followed by the completion of 151 guarded hot-box tests (Desjarlais and Tye, 1990) with analysis and correlations for the thermal resistance (Desjarlais and Yarbrough, 1991). The hot-box results cited above include thermal resistances (RSI values) for heat flow directions: up, 45° up, horizontal, 45° down, and down. The arrows in Figure 1 illustrate these directions with heat flow from warm surfaces to cool surfaces due to a temperature difference, ΔT, between parallel surfaces.

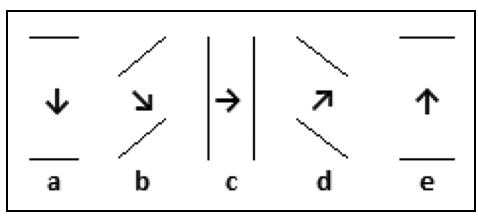

Figure 1. Heat flow from hot surface to cold surface shown for five directions: a—down, b—45° down, c—horizontal, d—45° up, and e—up.

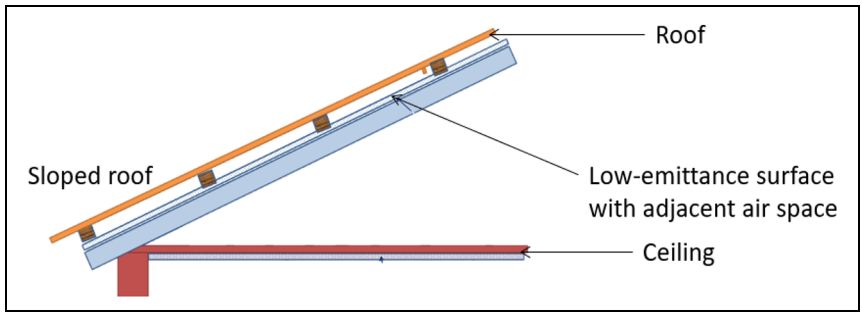

Figure 2. An example of a sloped enclosed reflective air space.

This article includes a new correlation for the convective component of the heat transfer across uniform thickness air spaces based on HRP 32 and the analytical approach described in an American Society for Testing and Materials (ASTM) Selected Technical Publication (STP) by Desjarlais and Yarbrough (1991). This analysis was undertaken to provide reliable RSI-values for the heat flow directions represented by the experimental data. These RSI-values become the fixed points for calculating (interpolating) results for heat flow down at various angles. The RSI-values at specific angles are needed for the accurate evaluation of U-values used in energy-use calculations and for the satisfaction of code requirements. Figure 2 is an example of an application that has a sloped air space.

Extracting data from HRP 32

The data forming the basis for the present analysis were obtained from a 400 by 500 mm graph prepared by Robinson et al. (1954). Numerical values, data points, were obtained by tracing the graphical presentation with a graphical digitizer (GetData Graph Digitizer 2.26, n.d.). There are five curves representing five heat flow directions, that is, down, 45° down, horizontal, 45° up, and up. Each curve was processed to obtain data points for $\log_{10} Nu$ as a function of $\log_{10} Gr$ with a resolution of ~0.01. A total of five tables were established; one for each heat flow direction. Table 1 contains, for example, 10 data points for heat flow 45° down, while Figure 3 shows data for heat flow 45° down.

Numerical data of the type shown in Table 1 and Figure 3 were collected for each heat flow direction. These data were then used to construct a three-segment smooth curve for each heat flow direction. In each case, Segment 1 is for $\log_{10} Nu$ equal 0 ($Nu = 1$, no convection), Segment 2 is a polynomial that describes the transition region, and Segment 3 is a polynomial for a region with increasing convective heat transport. The functions for each segment were described using the method of least squares subject to the conditions of continuity and continuous first derivative where the segments meet. These equations when combined with the

Table 1. Data for heat flow 45° down

$\log_{10}Gr$	$\log_{10}Nu$
3.750	0.0048
4.118	0.0304
4.401	0.0751
4.739	0.1665
5.070	0.2836
5.401	0.4123
5.734	0.5342
6.063	0.6407
6.391	0.7368
6.732	0.8271

Stefan–Boltzmann equation adjusted for net radiative transfer between parallel planes to calculate the heat flux across an air space between isothermal planes resulting from a temperature difference, ΔT, between them. Table 2 contains values for $\Delta T\, L^3$ below which convection is predicted to be absent.

Equations for $\log_{10}\, Nu$ for the three $\log_{10}\, Gr$ intervals are shown below. Table 3 contains values for the constants appearing in the equations. Equations (1a) to (1c) are used to calculate the convective component, equation (2) for $\log_{10}\, Gr$, and equation (7) for the thermal conductivity of air

$$\log_{10}Nu = 0 \;\; for \;\; \log_{10}Gr < \log_{10}Gr_0 \tag{1a}$$

$$\log_{10}Nu = a_2[\log_{10}Gr - \log_{10}Gr_0]^2 + a_3[\log_{10}Gr - \log_{10}Gr_0]^3 \quad \text{for } \log_{10}Gr_0 \leq \log_{10}Gr < \log_{10}Gr_1 \tag{1b}$$

$$\log_{10}Nu = a + b[\log_{10}Gr] + c[\log_{10}Gr]^2 \quad \text{for } \log_{10}Gr_1 \leq \log_{10}Gr < \log_{10}Gr_2 \tag{1c}$$

$$\log_{10}Gr = \log_{10}\left(\Delta T l^3\right) + 8.3196 - 0.007426 \cdot T_m + 0.000011807 \cdot T_m^2 \tag{2}$$

Calculation of RSI using the new correlation for *Nu*

$$RSI = \frac{1}{(h_r + h_{cc})} \tag{3}$$

$$h_r = 4 \cdot E \cdot \sigma \cdot T_m^3 \quad (T_m \text{ in } K) \tag{4}$$

$$E = \frac{1}{\left(\frac{1}{\varepsilon_1} + \frac{1}{\varepsilon_2} - 1\right)} \tag{5}$$

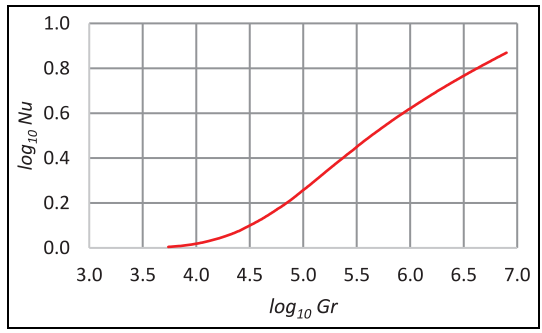

Figure 3. Curve for heat flow 45° down.

Table 2. Onset of convection

Heat flow direction	Maximum $\Delta T \cdot L^3$ (°C · cm^3)	
	T_m = 10°C	T_m = 27.5°C
Down	12.7	16.8
45° down	12.7	16.8
Horizontal	10.1	13.4
45° up	5.7	7.5
Up	1.4	1.9

Table 3. Constants for equations (1a) to (1c)

Heat flow direction	$Log_{10}Gr_0$	$Log_{10}Gr_1$	$Log_{10}Gr_2$	A	b	c	a_2	a_3
0° down	3.35	5.85	7.20	1.6517	−0.6418	0.0650	0.0110	0.0034
45° down	3.35	4.95	7.20	−2.7353	0.7992	−0.0400	0.0300	0.0400
Horizontal	3.25	4.35	7.20	−2.3207	0.7169	−0.0340	0.0000	0.1160
45° up	3.00	3.83	7.20	−1.2438	0.3877	−0.0070	0.2000	0.0010
0° up	2.40	3.50	7.20	−0.8440	0.2867	−0.0002	0.1295	0.0001

$$h_{cc} = Nu \cdot \left(\frac{k}{l}\right) \tag{6}$$

$$k = 0.02428 + 0.000070714 \cdot T_m \quad (T_m \text{ in } °C) \tag{7}$$

Equations (3) to (7) were used to calculate RSI_{New} for conditions in the table "Effective Thermal Resistance of Plane Air Spaces" in the 2017 edition of the ASHRAE Handbook Fundamentals. The calculated RSI-values are in good

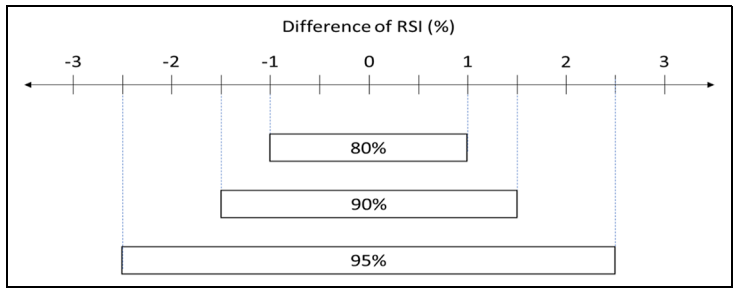

Figure 4. Range of percentage differences between the new correlation and the 2017 ASHRAE Handbook (% difference = $100 \cdot (RSI_{HB}–RSI_{New})/RSI_{New}$).

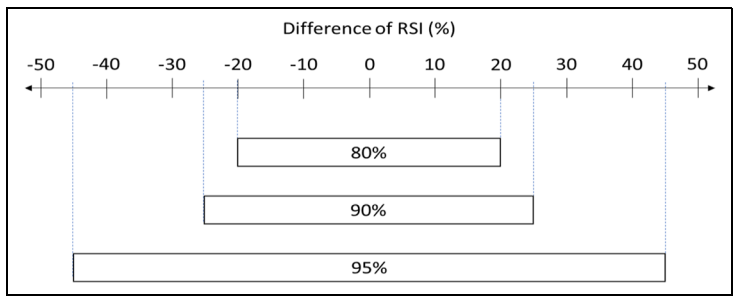

Figure 5. Range of percentage differences between the new correlation and ISO 6946 (% difference = $100 \cdot (RSI_{ISO}–RSI_{New})/RSI_{New}$).

agreement with those contained in the Handbook. The maximum difference between the RSI-values is $0.06\,m^2$ K/W with 95% of the values being within $\pm 2.5\%$ of the Handbook values. Figure 4 shows results for intervals containing 80%, 90%, or 95% of the data set. A similar comparison of RSI-values calculated using an International Standard (ISO 6946:2017, 2017) is contained in Figure 5. The RSI for heat flow 45° down is not included in the ISO standard. In total, 700 RSI-values from the two sources were compared with RSI-values differing by as much as $0.53\,m^2$ K/W. Figure 4 shows the large percentage difference required to contain 80%, 90%, or 95% of the RSI differences.

RSI values based on ISO 6946 have large differences mainly due to its simplified correlations for the conduction–convection coefficient, h_{cc}, which neglects the dependence of the thermal conductivity of air with temperature. Figures 6 to 8 compare the calculated RSI-values as a function of air gap size for the two sources.

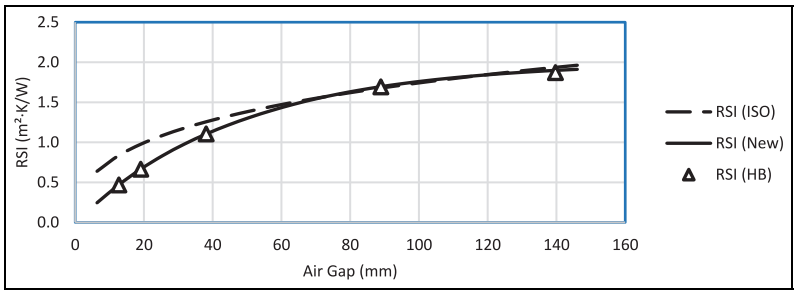

Figure 6. RSI for heat flow down ($E = 0.03$, $T_m = 10.0°C$, and $\Delta T = 16.7°C$).

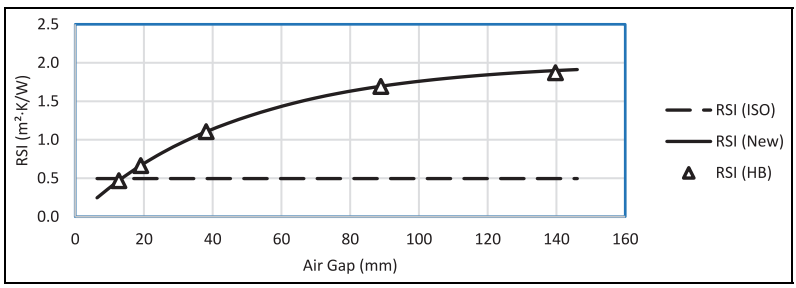

Figure 7. RSI for heat flow horizontal ($E = 0.03$, $T_m = 10.0°C$, $\Delta T = 16.7°C$).

Interpolation in heat flow direction (slope)

The RSI-values for air spaces with heat flow direction other than the five directions commonly tabulated can be expected to fall between the RSI-values of the bounding directions. Since radiation heat transfer between two parallel plains is independent of orientation, the interpolation is used to determine the conduction–convection coefficient, h_{cc}. The ISO standard suggests linear interpolation between heat flow horizontal and heat flow up to estimate intermediate h_{cc} but makes no recommendation for heat flow down. The objective in this article is the estimation of h_{cc} for heat flow direction between heat flow down and heat flow horizontal. Two interpolation equations were considered

$$h_{cc_\theta} = \left(h_{cc_0} \cdot \left(1 - \frac{\theta}{90}\right)\right) + \left(h_{cc_{90}} \cdot \frac{\theta}{90}\right) \tag{8}$$

and

$$h_{cc_\theta} = (h_{cc_0} \cdot (1 - \sin\theta)) + (h_{cc_{90}} \cdot \sin\theta). \tag{9}$$

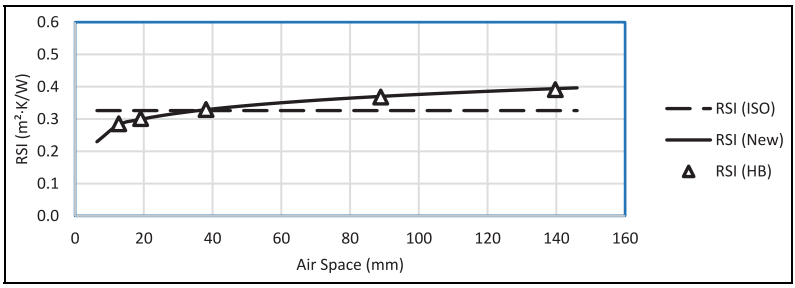

Figure 8. RSI comparison for heat flow up ($E = 0.03$, $T_m = 10.0°C$, $\Delta T = 16.7°C$).

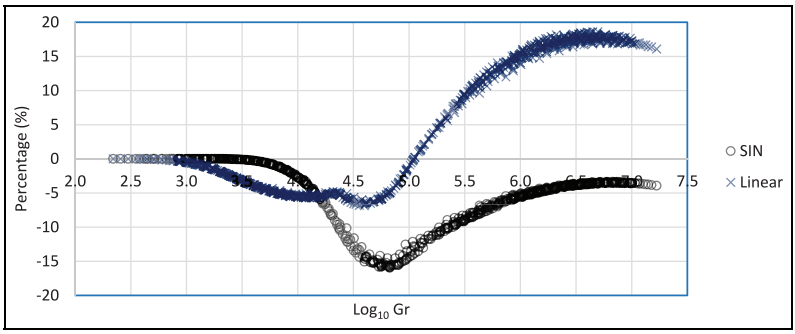

Figure 9. Percentage difference between interpolated and measured RSI-values for 45° down.

Table 4. Air gap conditions included in analyses

Conditions	Units	Values
Mean temperature	°C	−10, 0, 10, 20, 30, 40
Temperature difference	°C	2, 4, 6, 8, 10, 12, 14, 16, 18, 20
Air gap	mm	10, 12, 15, 20, 30, 50, 75, 100, 125, 150

Equation (8) is linear interpolation, while equation (9) includes $\sin(\theta)$ suggested by a force balance. These interpolation equations were used to evaluate RSI-values for heat flow 45° down by interpolating between $\theta = 0$ and 90°. The RSI for the 600 air gap combinations in Table 4 that include $\log_{10} Gr$ ranging from 2.3 to 7.2 was obtained with equations (8) and (9) and compared with RSI-values calculated using equation (3).

Figure 9 shows the percentage difference between interpolated RSI-values and RSI from test data represented by equation (3). RSI-values obtained using linear

Table 5. RSI-values for heat flow down

		RSI of reflective air spaces for heat flow down ($T_m = 27.5°$, $E = 0.05$, $\Delta T = 15°C$)									
		Air gap (mm)									
		5	10	15	20	25	30	35	40	45	50
Angle (°)	0	0.18	0.34	0.48	0.61	0.71	0.80	0.88	0.96	1.02	1.07
	5	0.18	0.34	0.48	0.60	0.70	0.78	0.85	0.90	0.95	0.99
	10	0.18	0.34	0.48	0.60	0.69	0.76	0.81	0.85	0.89	0.91
	15	0.18	0.34	0.48	0.59	0.68	0.74	0.78	0.81	0.83	0.85
	20	0.18	0.34	0.48	0.59	0.67	0.72	0.75	0.77	0.78	0.80
	25	0.18	0.34	0.48	0.58	0.66	0.70	0.72	0.73	0.74	0.75
	30	0.18	0.34	0.48	0.58	0.64	0.68	0.70	0.70	0.70	0.70
	35	0.18	0.34	0.48	0.57	0.63	0.67	0.67	0.67	0.67	0.67
	40	0.18	0.34	0.48	0.57	0.62	0.65	0.65	0.64	0.64	0.63
	45	0.18	0.34	0.48	0.57	0.62	0.63	0.63	0.62	0.61	0.60

interpolation showed a maximum difference of 19% from the test data, while the interpolation based on $\sin(\theta)$ showed a 16% maximum difference. Both models showed unacceptable deviations from equation (3). As a result, an interpolation between the measured values at 0°, 45°, and 90° represented by equations (10a) and (10b) termed a bilinear model is introduced

$$h_{cc_\theta} = \left(h_{cc_0} \cdot \left(1 - \frac{\theta}{45}\right)\right) + \left(h_{cc_{45}} \cdot \frac{\theta}{45}\right) \quad \text{for } 0° < \theta < 45° \tag{10a}$$

$$h_{cc_\theta} = \left(h_{cc_{45}} \cdot \left(1 - \frac{\theta - 45}{45}\right)\right) + \left(h_{cc_{90}} \cdot \frac{\theta - 45}{45}\right) \quad \text{for } 45° < \theta < 90° \tag{10b}$$

RSI-values calculated with the bilinear model are not smooth at 45°; there is a discontinuity in the slope that does not significantly affect calculated RSI-values. Figure 10 shows RSI-values from linear interpolation, interpolation based on $\sin(\theta)$, and the bilinear model. The curves in Figure 9 show that linear interpolation or the $\sin(\theta)$ model between 0° and 90° does not provide satisfactory results at 45°. Figure 11 is a similar comparison for air gap of 150 mm. The free convection component of the heat flow is much larger at 150 mm than it is at 25 mm and the $\sin(\theta)$ interpolation is correct at 45°. The bilinear, however, is selected as a practical solution for the most engineering applications and is recommended for applications requiring RSI-values for enclosed reflective air spaces below sloped roofs. Table 5 is provided as an example of RSI variation with slope of an enclosed reflective air space below a roof. The RSI-values for heat flow down, heat flow down at 45°, and heat flow horizontal can be obtained from equations (1) to (7) and used for interpolations for any angle with heat flow down.

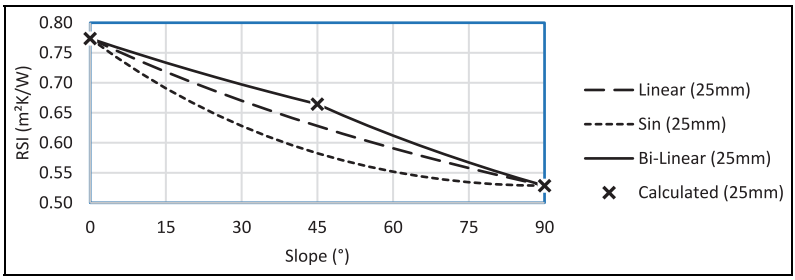

Figure 10. RSI versus slope for a 25 mm air gap (heat flow down, $E = 0.03$, $T_m = 30°C$, $\Delta T = 15°C$).

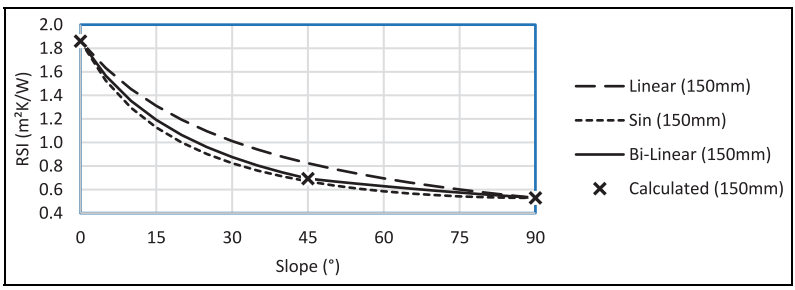

Figure 11. RSI versus slope for a 150 mm air gap (heat flow down, $E = 0.03$, $T_m = 30°C$, $\Delta T = 15°C$).

Conclusion and recommendation

A systematic analysis of previously published thermal data has resulted in smooth equations that provide *Nu* as a function of *Gr* over a wide range of conditions and *Gr* up to $\sim 10^7$.

RSI for downward heat flow ($\theta = 0$), 45° down, and horizontal is especially important since these values anchor the interpolations to calculate RSI at intermediate slopes.

The constants in Table 3 are recommended for the calculation of *Nu* for enclosed reflective air spaces using equations (1) and (2). The new parameters agree with the table of values contained in the 2017 edition of the ASHRAE Handbook of Fundamentals and the data in HRP 32 to within ± 2.5%.

The results from equations (1) and (2) along with interpolation using equation (9) provide for the calculation of the thermal resistances of large parallel spaces bounded by isothermal surfaces at any orientation from heat flow down (horizontal roof) to heat flow horizontal (a wall).

Acknowledgements

The authors thank San Miguel Yamamura Woven Products and Mr T.S. Tan for providing encouragement and resources for this study.

Declaration of conflicting interests

The author(s) declared no potential conflicts of interest with respect to the research, authorship, and/or publication of this article.

Funding

The author(s) received no financial support for the research, authorship, and/or publication of this article.

ORCID iD

David W Yarbrough https://orcid.org/0000-0001-6383-4385

References

American Society of Heating, Refrigerating and Air-Conditioning Engineers (ASHRAE) (1972) *ASHRAE Handbook Fundamentals*. Atlanta, GA: ASHRAE, pp. 357–360.

American Society of Heating, Refrigerating and Air-Conditioning Engineers (ASHRAE) (2017) *ASHRAE Handbook Fundamentals*. Atlanta, GA: ASHRAE, pp. 2614–2615.

Desjarlais AO and Tye RP (1990) *Research and development data to define the thermal performance of reflective materials used to conserve energy in building applications*. Oak Ridge National Laboratory report no. ORNL/Sub/88-SA835/1, 1 March. Oak Ridge, TN: Oak Ridge National Laboratory.

Desjarlais AO and Yarbrough DW (1991) Prediction of the thermal performance of single and multi-airspace reflective insulation materials. In: Graves RS and Wysocki DC (eds) *Insulation Materials: Testing and Applications* (ASTM STP 1116), vol. 2. West Conshohocken, PA: American Society for Testing and Materials, pp. 24–43.

GetData Graph Digitizer 2.26 (n.d.) Available at: http://getdata-graph-digitizer.com/download.php

Goss WP and Miller RG (1989) Literature review of measurement and predictions of reflective building insulation system performance, 1900-1989. *ASHRAE Transactions* 95(Pt 2): 651–664.

ISO 6946: 2017 (2017) Building components and building elements—thermal resistance and thermal transmittance—calculation methods (3rd ed., Annex D: thermal resistance of airspaces).

Lee SW, Lim CH and Salleh IB (2016) Reflective thermal insulation systems in building: a review on radiant barrier and reflective insulation. *Renewable & Sustainable Energy Reviews* 65: 643–661.

Robinson HE and Powell FJ (1956) *The thermal insulating value of air spaces*. Housing research paper no. 32. April. Washington, DC: Home Finance Agency, US Government Printing Office.

Robinson HE, Powlitch FJ and Dill RS (1954) *The thermal insulating value of air spaces*. National Bureau of Standards report 3030, 11 January. Washington, DC: United States Department of Commerce, National Bureau of Standards.

Saber HH (2014) Practical correlation for thermal resistance of low-sloped enclosed airspaces with downward heat flow for building applications. *HVAC&R Research* 20(1): 92–112.

Saber HH, Maref W, and Hajiah A (2020) *Effective R-values of Enclosed Reflective Space for Different Building Applications, J. Building Physics* 43(5): 398–427.

Appendix 1

Notation

E	effective emittance	defined by equation (5)
g	acceleration due to gravity	m/s^2
Gr	Grashof number ($\Delta T\, l^3\, \beta\, g/\upsilon^2$)	dimensionless
h	heat transfer coefficient	$W/m^2 \cdot K$
h_{cc}	heat transfer coefficient for conduction–convection	
h_r	heat transfer coefficient for radiation	
k	thermal conductivity	$W/m \cdot K$
l	length or distance	m
Nu	Nusselt number ($h \cdot l/k$) dimensionless	
RSI	thermal resistance with SI units	$m^2 \cdot K/W$
T	temperature	°C, K
T_m	mean or average temperature	°C, K
β	temperature coefficient of volume expansion	$1/T$, K^{-1}
ΔT	temperature difference across air space	°C, K
ϵ	total hemispherical emittance	dimensionless
θ	angle of incidence	0 is horizontal, heat flow down
σ	Stefan–Boltzmann constant	$W/m^2 \cdot K^4$
υ	kinematic viscosity	m^2/K